2007 IEEE International Conference on
Robotics and Automation
Roma, Italy, 10-14 April 2007

Curvilinear Transport of Suspended Payloads *

C. Williams, G. Starr, J. Wood, and R. Lumia
Department of Mechanical Engineering
The University of New Mexico
Albuquerque, New Mexico 87131, USA
christine.a.williams@gmail.com, (starr,wood,lumia)@me.unm.edu

***Abstract*— Automated transport of suspended objects is a subject of importance in many manufacturing, construction, and military applications. Suppression of the natural oscillation of payloads after a transport motion has been extensively studied, but generalized planar motion has yet to be examined. Obstacles in a crane or robot workspace may necessitate transport using a sequence of many linear segments or by a sequence of fewer curvilinear ones. The use of curvilinear motions in such cases may have the following advantages: (1) less error build-up in optimization due to the use of fewer segments, and (2) faster transport. We investigate parametrically-defined polynomial spatial paths optimized using dynamic programming. We present simulations and experimental evaluations of these optimizations.**

I. Introduction

In transporting suspended objects, it is often desired that oscillations of the payload be suppressed at the end of a transport maneuver. This is an area of interest for many industries, including manufacturing plants, construction, and the military.

Past research has been concerned with various methods of optimizing linear trajectories, where the issue of obstacle avoidance may require splining together multiple trajectories [1]. Depending on the complexity of the path required to avoid collisions, this can greatly increase the total transport time. The use of curvilinear trajectories can reduce transport time and adds greater flexibility in motion planning.

Parametrically-defined trajectories are necessary for this work because they allow for simultaneous optimization of multiple dimensions of motion. By optimizing a single parameter, a specific spatial path can be maintained, something that would not be possible if x and y motions were optimized independently. The method of dynamic programming, used in swing-free research due to its applicability to non-linear systems, can be used to successfully suppress residual oscillations of a payload transported along curvilinear paths.

A. Impulse-Convolution and Parameter Optimization

Two methods that have been used frequently in swing-free research are impulse-convolution and parameter optimization. Suppression of residual oscillation using command trajectories was first investigated by Smith [2] and further developed by Starr [3] and Strip [4]. The work of Singer and Seering [5] was the beginning of the impulse-convolution method, an open-loop control technique wherein a sequence of impulses is convolved with a desired trajectory in order to minimize residual vibrations. This work has been extensively explored and applied to two-mode systems [6], container crane systems [7], and many other applications.

Parameter optimization is another frequently-used method of suppressing residual motion. Utilizing basis functions (usually "bang-coast-bang" piecewise functions) and quadratic programming, this method has been applied to vibration suppression of flexible rods [8], jib cranes [9], and other systems.

While both of these methods have been successfully used in swing-free research, they are not without their drawbacks. Impulse-convolution requires linearization of non-linear systems. This limitation eliminates most high-speed transport maneuvers because they generate large swing angles, making small-angle linearizing assumptions invalid. It also has a tendency to generate non-smooth velocity profiles. A problem with parameter optimization is that an accurate initial estimate of the trajectory parameters may be required to converge to a truly optimal solution. These issues are discussed in greater detail by Starr *et al* [10].

B. Dynamic Programming

Dynamic Programming can avoid many of the aforementioned problems. It is based on the principle of optimality and was first developed by Bellman [11]. Using the approach of Robinett *et al* [12], Starr *et al* [3] chose objective function matrices to enforce a minimum energy condition for the optimization of movements by a gantry crane system with one degree of freedom. We have applied this same methodology to a two degree of freedom extension of the system for investigating curvilinear motions.

II. System and Trajectory Formulation

A. System and Trajectory Modeling

The system used for our investigation is a simple pendulum modeled as a two degree of freedom system with a 2-1 Euler angle rotation sequence, depicted in Fig. 1. While this rotation sequence does have singularities, they occur when $\phi = \pm\pi$ radians, far beyond the range of motion seen in our simulations or experiments. Equations of motion for the

*This work is supported by US DOE Grant #DE-FG52-04NA25590 awarded to the UNM Manufacturing Engineering Program

system are as follows:

$$\ddot{\theta} = 2\dot{\theta}\dot{\phi}\tan\phi - \frac{g}{l}\frac{\sin\theta}{\cos\phi} + \frac{1}{l}\ddot{x}\frac{\cos\theta}{\cos\phi} \quad (1)$$

$$\ddot{\phi} = -\dot{\theta}^2\cos\phi\sin\phi - \frac{g}{l}\cos\theta\sin\phi - \frac{1}{l}(\ddot{x}\sin\theta\sin\phi + \ddot{y}\cos\phi). \quad (2)$$

Fig. 1. 2-1 Euler Angle Rotation

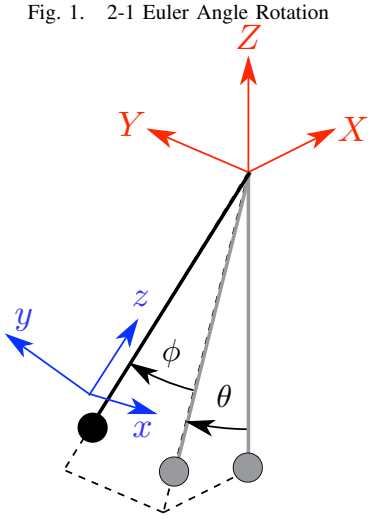

Initially, we considered elliptical spatial trajectories for this work. However, an angle of inclination and exactly four points must be used to define elliptical segments, and only a small fraction of possible point sets can be used to define an ellipse. In addition, for spatial slope continuity between splined segments, the proper angle of inclination for the next elliptical arc in the sequence must be found iteratively.

For these reasons, polynomial trajectories were considered as an alternative to elliptical arcs. Unlike ellipses, polynomials can be defined by as few as two spatial coordinates (linear). The maximum number of coordinates that can be used to define a polynomial depends on the specific coordinates used. Some generate polynomials with undesirable higher-order behavior, but we have used as many as ten coordinates to define a reasonable polynomial in examining possible trajectories. Polynomials also allow the spatial derivatives at the end points to be explicitly defined.

The polynomial spatial formulation is:

$$x(\gamma) = \sum_{i=0}^{n} a_i\gamma^i \quad (3)$$

$$y(\gamma) = \sum_{i=0}^{n} b_i\gamma^i, \quad (4)$$

where γ is defined as:

$$\gamma_1 = 0 \quad (5)$$

$$\gamma_j = \gamma_{j-1} + \sqrt{(X_j - X_{j-1})^2 + (Y_j - Y_{j-1})^2}. \quad (6)$$

The set of points X_j, Y_j are those through which the polynomial must pass. An n^{th} order polynomial so constrained will pass through $n+1$ points. If the derivatives of the polynomial at its end points needs to be explicitly defined, additional contraints will apply and an n^{th} order polynomial will only pass through n points:

$$\left(\frac{dy}{dx}\right)_{\gamma=0} = \frac{b_1}{a_1} \quad (7)$$

$$\left(\frac{dy}{dx}\right)_{\gamma=\gamma_n} = \frac{\sum_{i=1}^{n} i b_i \gamma^{i-1}}{\sum_{i=1}^{n} i a_i \gamma^{i-1}}. \quad (8)$$

Optimization using dynamic programming requires system discretization in state-variable form. For the purposes of this research, we first constructed the system in the continuous domain and then discretized it. The continuous state-variable system, as derived from equations of motion (1)-(2) and parametric equations (4)-(5) is given by:

$$\dot{\mathbf{x}}(t) = \mathbf{A}(t)\mathbf{x}(t) + \mathbf{B}(t)u(t), \quad (9)$$

where

$$\mathbf{x}(t) = \begin{bmatrix}\theta & \dot{\theta} & \phi & \dot{\phi} & \gamma & \dot{\gamma}\end{bmatrix}^T, \quad (10)$$

$$\mathbf{A}(t) = \begin{bmatrix} 0 & 1 & 0 & 0 & \dots \\ -\frac{g}{l}\frac{\mathrm{sinc}x_1}{c_3} & 2x_4\tan x_3 & 0 & 0 & \\ 0 & 0 & 0 & 1 & \\ 0 & -s_3c_3x_2 & -\frac{g}{l}c_1\mathrm{sinc}x_3 & 0 & \\ 0 & 0 & 0 & 0 & \\ 0 & 0 & 0 & 0 & \dots \end{bmatrix}$$

$$\begin{matrix} \dots & 0 & 0 \\ & 0 & \frac{1}{l}\frac{c_1}{c_3}\sum_{i=2}^{n} i(i-1)a_i x_5^{i-2}x_6 \\ & 0 & 0 \\ & 0 & \frac{-1}{l}\sum_{i=2}^{n} i(i-1)(a_i s_1 s_3 + b_i c_3)x_5^{i-2}x_6 \\ & 0 & 1 \\ \dots & 0 & 0 \end{matrix}, \quad (11)$$

and

$$\mathbf{B}(t) = \begin{bmatrix} 0 \\ \frac{1}{l}\frac{c_1}{c_3}\sum_{i=1}^{n} i a_i x_5^{i-1} \\ 0 \\ \frac{-1}{l}\sum_{i=1}^{n} i(a_i s_1 s_3 + b_i c_3)x_5^{i-1} \\ 0 \\ 1 \end{bmatrix}. \quad (12)$$

The input $u(t) = \ddot{\gamma}(t)$, is the parameter acceleration. As usual, s_1 means $\sin x_1$, c_5 means $\cos x_3$, *etc.*

B. Optimization using Dynamic Programming

Following the approach of [10], the equations of motion (9)–(12) were discretized to form (13), and an objective function Γ was formed which is quadratic in both the input and state:

$$\mathbf{x}_{k+1} = \mathbf{A}_k \mathbf{x}_k + \mathbf{B}_k \mathbf{u}_k \tag{13}$$

and

$$\Gamma(\mathbf{x}, \mathbf{u}) = \sum_{k=1}^{N} \Gamma_k(\mathbf{x}_k, \mathbf{u}_k) \tag{14}$$

where

$$\begin{aligned}\Gamma_k &= \eta_k + \mathbf{x}_k^T \mathbf{y}_k + \mathbf{u}_k^T \mathbf{z}_k \\ &\quad + \frac{1}{2}\left[\mathbf{x}_k^T \mathbf{Q}_k \mathbf{x}_k + 2\mathbf{x}_k^T \mathbf{R}_k \mathbf{u}_k + \mathbf{u}_k^T \mathbf{S}_k \mathbf{u}_k\right]\end{aligned} \tag{15}$$

Note that the quadratic objective function structure of (15) is most general; in the particular application of this paper the weighting sequences $\eta_k, \mathbf{y}_k, \mathbf{z}_k, \mathbf{Q}_k, \mathbf{R}_k$ are all zero.

Define the optimal value function Λ_i as

$$\Lambda_i = \min_{(\mathbf{u}_i \cdots \mathbf{u}_N)} \sum_{k=i}^{N} \Gamma_k(\mathbf{x}_k, \mathbf{u}_k) \tag{16}$$

Thus Λ_i represents the optimal objective function sequence from intermediate sample i to final sample N.

One can express this quadratic optimal value function as

$$\Lambda_i = \zeta_i + \mathbf{x}_i^T \mathbf{v}_i + \frac{\mathbf{x}_i^T \mathbf{W}_i \mathbf{x}_i}{2}. \tag{17}$$

Note that Λ_i is a function only of $\mathbf{x}_i$.

The principle of optimality may be stated as the backwards recursion relation

$$\Lambda_i = \min_{\mathbf{u}_i} \Gamma_i + \Lambda_{i+1} \tag{18}$$

Substituting (15), (16), and (17) into (18) yields the recursive relation

$$\begin{aligned}&\zeta_i + \mathbf{x}_i^T \mathbf{v}_i + \frac{\mathbf{x}_i^T \mathbf{W}_i \mathbf{x}_i}{2} = \\ &\quad \zeta_{i+1} + \mathbf{x}_{i+1}^T \mathbf{v}_{i+1} + \frac{\mathbf{x}_{i+1}^T \mathbf{W}_{i+1} \mathbf{x}_{i+1}}{2} \\ &\quad + \min_{\mathbf{u}_i} \left\{ \eta_i + \mathbf{x}_k^T \mathbf{y}_k + \mathbf{u}_k^T \mathbf{z}_k \right. \\ &\quad \left. + \frac{1}{2}\mathbf{x}_k^T \mathbf{Q}_k \mathbf{x}_k + 2\mathbf{x}_k^T \mathbf{R}_k \mathbf{u}_k + \mathbf{u}_k^T \mathbf{S}_k \mathbf{u}_k \right\}\end{aligned} \tag{19}$$

Introducing state equation (13) into (19) leads to

$$\begin{aligned}&\zeta_i + \mathbf{x}_i^T \mathbf{v}_i + \frac{\mathbf{x}_i^T \mathbf{W}_i \mathbf{x}_i}{2} = \zeta_{i+1} + \eta_i + \mathbf{x}_i^T \mathbf{h}_{4i} \\ &\quad + \min_{\mathbf{u}_i} \left\{ \mathbf{u}_i^T \mathbf{h}_{5i} + \frac{\left[\mathbf{x}_i^T \mathbf{H}_{1i} \mathbf{x}_i + 2\mathbf{x}_i^T \mathbf{H}_{2i} \mathbf{u}_i + \mathbf{u}_i^T \mathbf{H}_{3i} \mathbf{u}_i\right]}{2} \right\}\end{aligned} \tag{20}$$

where we have consolidated terms

$$\begin{aligned}\mathbf{H}_{1i} &= \mathbf{Q}_i + \mathbf{A}_i^T \mathbf{W}_{i+1} \mathbf{A}_i \\ \mathbf{H}_{2i} &= \mathbf{R}_i + \mathbf{A}_i^T \mathbf{W}_{i+1} \mathbf{B}_i \\ \mathbf{H}_{3i} &= \mathbf{S}_i + \mathbf{B}_i^T \mathbf{W}_{i+1} \mathbf{B}_i \\ \mathbf{h}_{4i} &= \mathbf{y}_i + \mathbf{A}_i^T \mathbf{v}_{i+1} \\ \mathbf{h}_{5i} &= \mathbf{z}_i + \mathbf{B}_i^T \mathbf{v}_{i+1}\end{aligned}$$

Differentiating the lower expression in (20) with respect to $\mathbf{u}_i$ and equating to zero yields

$$\mathbf{u}_i = -\mathbf{H}_{3i}^{-1}\left[\mathbf{H}_{2i}\mathbf{x}_i + \mathbf{h}_{5i}\right]. \tag{21}$$

Finally, substitution of $\mathbf{u}_i$ from (21) into (20) and equating coefficients of like degree in $\mathbf{x}_i$ produces the following recursive equations:

$$\zeta_i = \zeta_{i+1} + \eta_i - \frac{\mathbf{h}_{5i}^T \mathbf{H}_{3i}^{-1} \mathbf{h}_{5i}}{2} \tag{22}$$

$$\mathbf{v}_i = \mathbf{h}_{4i} - \mathbf{H}_{2i} \mathbf{H}_{3i}^{-1} \mathbf{h}_{5i} \tag{23}$$

$$\mathbf{W}_i = \mathbf{H}_{1i} - \mathbf{H}_{2i} \mathbf{H}_{3i}^{-1} \mathbf{H}_{2i}^T. \tag{24}$$

The initial values for (14)-(16) are given by

$$\zeta_N = \eta_N \tag{25}$$

$$\mathbf{v}_N = \mathbf{y}_N \tag{26}$$

$$\mathbf{W}_N = \mathbf{Q}_N. \tag{27}$$

Summary of Algorithm. The procedure for applying the dynamic programming algorithm is as follows:

1) Calculate $\mathbf{v}_N$ and $\mathbf{W}_N$ using (18 and (19).
2) Calculate $\mathbf{v}_i$ and $\mathbf{W}_i$ recursively for $i = N-1$ to $i = 1$ by using (15) and (16) and store the matrices $\mathbf{H}_{3i}^{-1}$, $\mathbf{H}_{2i}^T$, and $\mathbf{H}_{3i}^{-1}\mathbf{h}_{5i}$ in the process.
3) Calculate $\mathbf{u}_i$ and $\mathbf{x}_i$ recursively for $i = 1$ to $i = N-1$ by using (13) and (5), respectively.

It should be noted that a single complete execution of the above dynamic program is deterministic, with computational features:

1) Order Nn^3 operations are required,
2) Order Nnm storage is required.

C. Application to Curvilinear Transport

The dynamic behavior of the suspended body is given by (9)–(12), where the input in (9) is trajectory parameter acceleration $\ddot{\gamma}$.

The objective function matrices were

$$\begin{aligned}\mathbf{Q}_k &= \mathbf{0} \\ \mathbf{R}_k &= \mathbf{0} \\ \mathbf{S}_k &= \mathbf{I}_n\end{aligned}$$

which enforced a minimum-energy condition.

To suppress residual oscillation while achieving the desired transport the final state must be (refer to (10)):

$$\mathbf{x}_F = \begin{bmatrix}0 & 0 & 0 & 0 & \gamma_F & 0\end{bmatrix}^T. \tag{28}$$

This final constraint was enforced by adjoining it to the objective function *via* a penalty weight p:

$$\Gamma = \sum_{k=1}^{N} \left\{ \frac{1}{2} u_k^2 + p \left[\mathbf{x}_N - \mathbf{x}_F \right]^T \left[\mathbf{x}_N - \mathbf{x}_F \right] \right\} \qquad (29)$$

III. Examples

Four spatial trajectories were examined in simulation and experiment: two short trajectories with path lengths Δs of 3.12 and 2.28 meters, respectively, and two long trajectories with Δs 6.12 and 6.09 meters. The two long trajectories were both comprised of shorter trajectories splined together at a via point. With the 6.12 meter path, no derviative constraints were applied at the endpoints, leading to a slope discontinuity at the via point. Because of this, the trajectory was constrained in the DP optimization have to zero velocity at the via point. In the 6.09 meter trajectory, slope constraints were applied so that there could be a non-zero velocity at the via point without generating any velocity discontinuities. These four trajectories are depicted in Fig. 2 through 5, along with the points in the workspace that were used to define the spatial path using the polynomial formulation described previously. Fig. 4 and 5 also depict closer views of the via points to show the difference that results when slope continuity is enforced.

Fig. 2. Short Polynomial #1 - 3.12 meters long

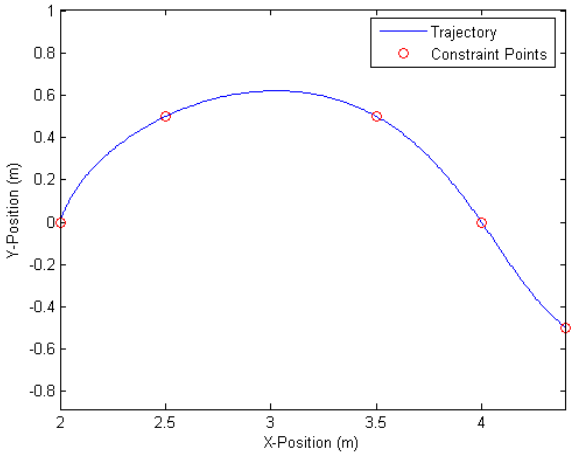

A. ADAMS Simulations

Both unoptimized and DP optimized trajectories were simulated in MSC.ADAMS, with a model depicted in Fig. 6. For the unoptimized trajectories, the $\gamma(t)$ functions used were cubic polynomials; these allow specification of endpoint position and velocity without excessive slewing speed. Three iterations of the DP optimization algorithm were used, with a time step Δt = 8 ms. For all trajectories, including both unoptimized and optimized cases, an average path speed $|v|_{avg}$ = 0.5 m/s was used, as this was fast enough to generate significant swing in transit, but slow enough to not exceed the limitations of the hardware used for experimental validation of the procedure.

Fig. 3. Short Polynomial #2 - 2.28 meters long

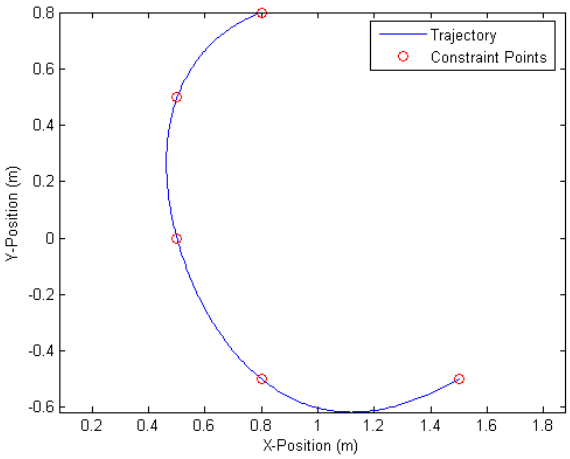

Fig. 4. Long Polynomial #1 - 6.12 meters long

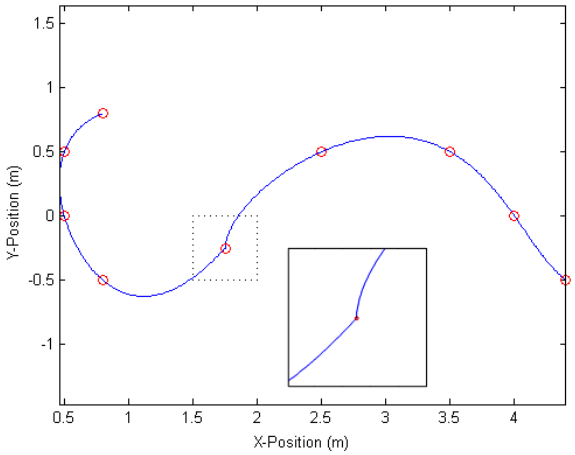

Fig. 5. Long Polynomial #2 - 6.09 meters long

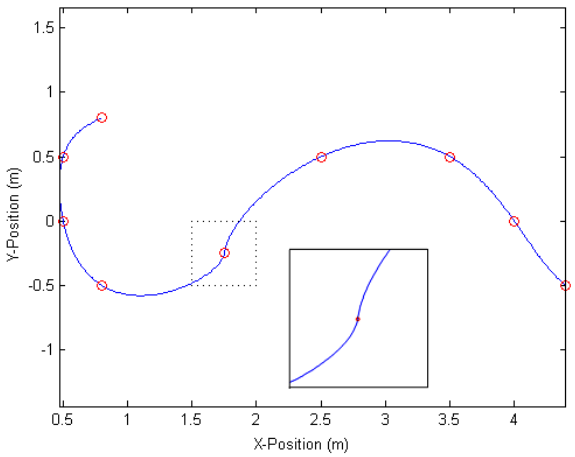

Fig. 7 through 10 depict the swing angles as predicted by the ADAMS simulations. $t_f = \Delta s / v_{avg}$ depicted in these figures is the time at which the motion of the pendulum pivot point stops. For an ideal swing-free case, the angles θ and ϕ should not change after that time. Table I lists numerical values of the residual swing amplitudes for both unoptimized (Unop.) and DP optimized (Op.) cases and percent reduction in swing with optimization. The average percent reduction was found to be 94.5%.

Fig. 6. Pendulum as modeled in MSC.ADAMS.

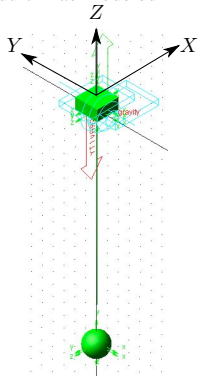

Fig. 7. Short Polynomial #1

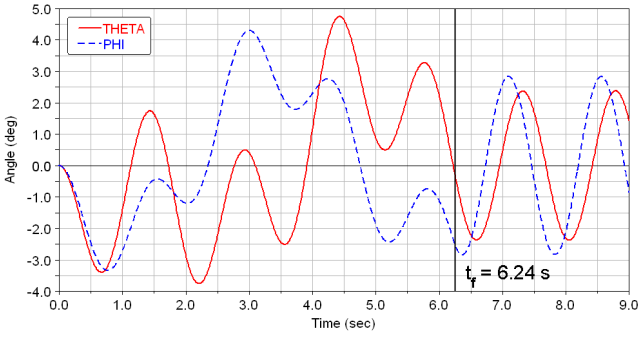

(a) Unoptimized

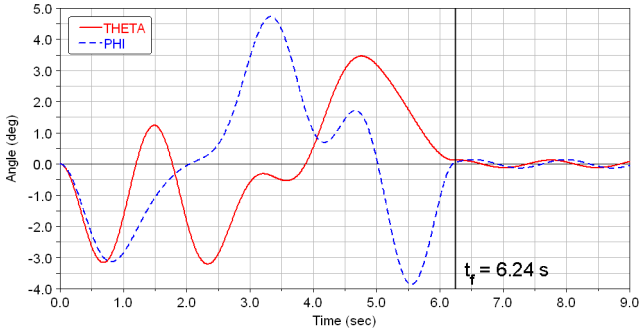

(b) DP Optimized

B. Experimental Validation

Experimentally, the system under investigation consists of a Staübli RX-130 manipulator from which slender cable and a small lead weight is suspended, depicted in Fig. 11.

Fig. 8. Short Polynomial #2

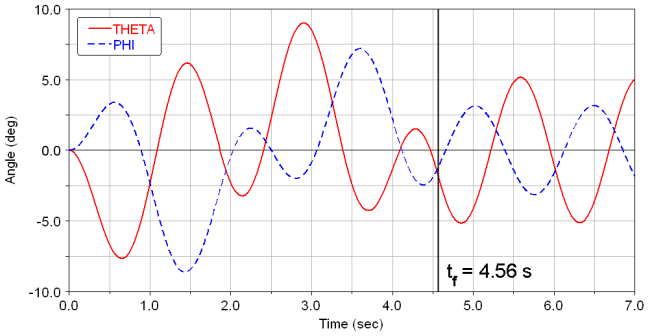

(a) Unoptimized

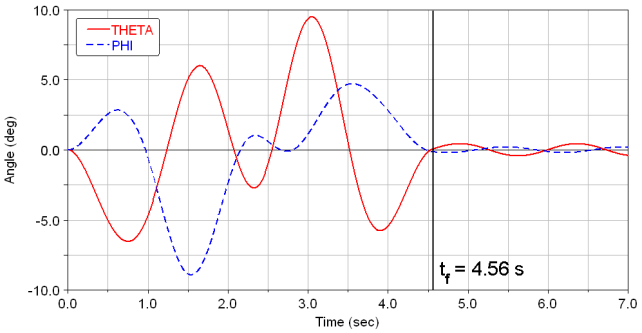

(b) DP Optimized

Fig. 9. Long Polynomial #1

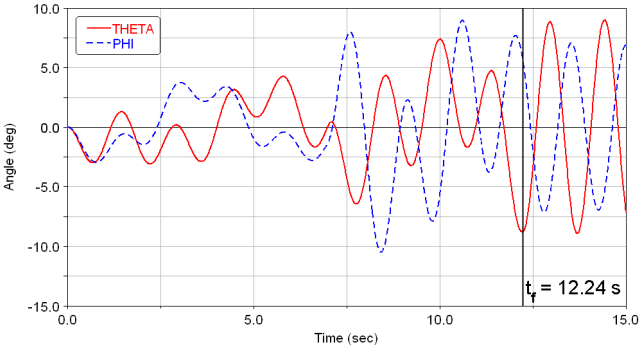

(a) Unoptimized

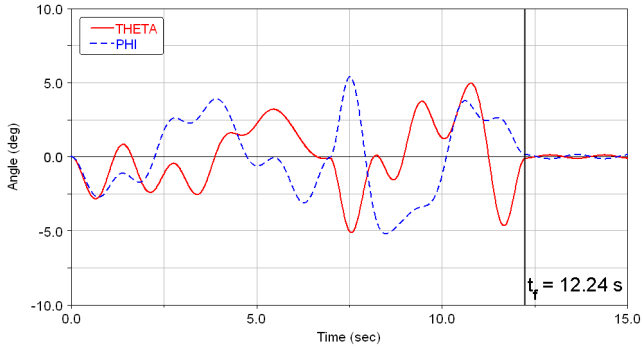

(b) DP Optimized

Fig. 10. Long Polynomial #2

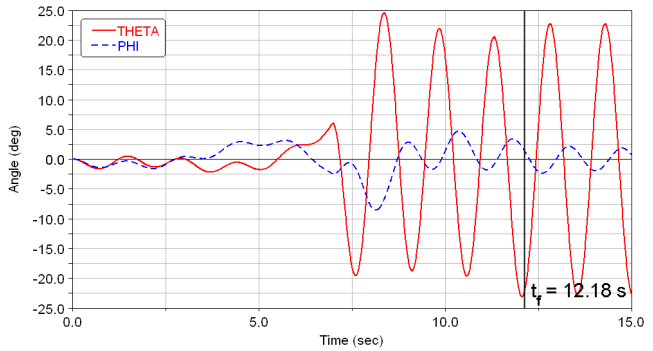

(a) Unoptimized

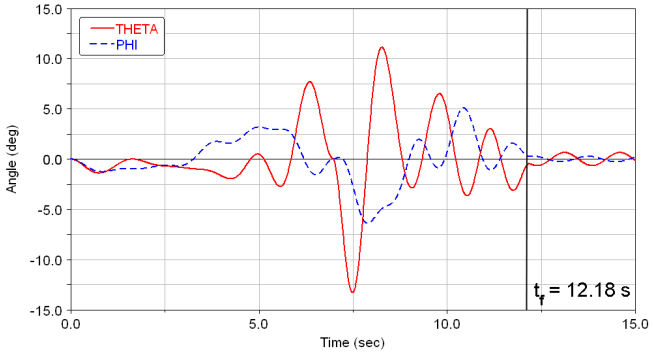

(b) DP Optimized

TABLE I
RESIDUAL SWING AMPLITUDES: SIMULATION

Traj.	Ang.	Unop. (deg)	Op. (deg)	Reduc. (%)
Short Poly. 1	θ	2.376	0.1221	94.9
	ϕ	2.837	0.1353	95.2
Short Poly. 2	θ	5.147	0.4327	91.6
	ϕ	3.159	0.2029	93.6
Long Poly. 1	θ	8.993	0.1173	98.7
	ϕ	7.058	0.1466	97.9
Long Poly. 2	θ	22.75	0.6527	97.2
	ϕ	2.14	0.2797	86.9

Fig. 11. Staübli RX-130 and RTU

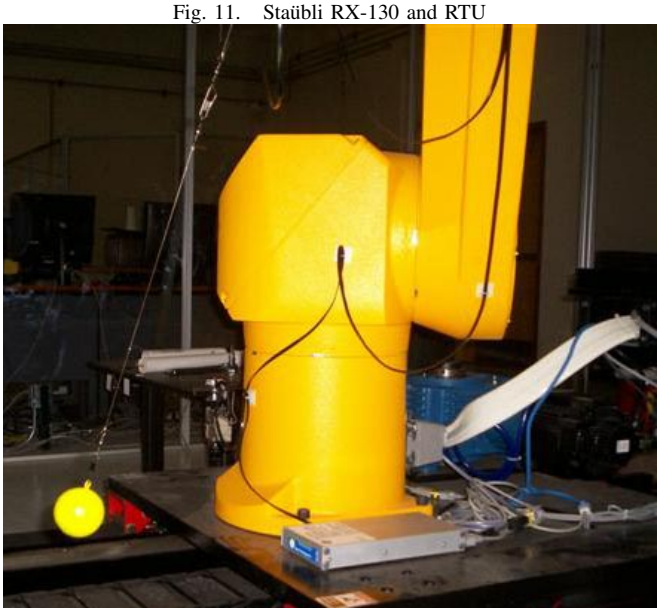

(a) A photograph of the Staübli RX-130 and payload taken at the end of a 6.09 meter transport maneuver.

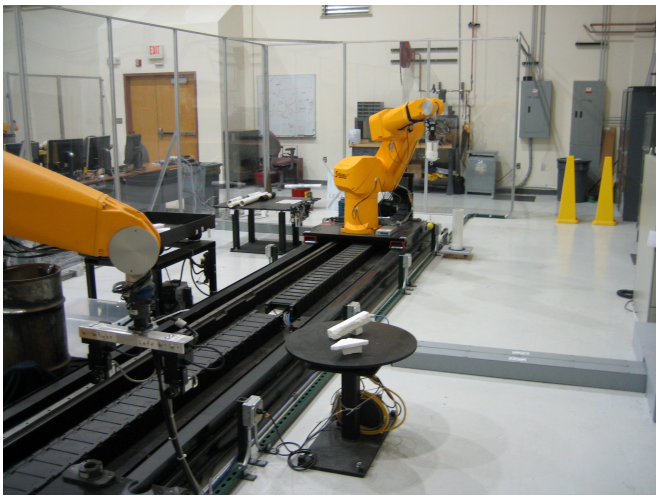

(b) Robot Transport Unit and two Staübli RX-130s.

The pendulum length was $l = 0.528$ meters. The Staübli, in conjunction with a translating Robot Transport Unit (RTU), is used to perform maneuvers that mimic those that industrial cranes can perform.

To test the effectiveness of the method, the aforementioned trajectories were sampled at a time step of $\Delta t = 16$ ms to match the sampling period of the Staübli RX-130's controller. The motion was apportioned between the Staübli and RTU. All motion in the y-direction was conducted by the Staübli; most of the motion in the x-direction was performed by the RTU, but some was done by the Staübli to avoid exceeding the RTU's speed limit.

Because we had no explicit angle sensors available to us, JR3 force sensors on the wrist of the robot were used to take measurements of the residual motion. From the force measurements, we were able determine the residual swing amplitudes in the x- and y-directions. Using inverse kinematics, these measurements were then used to determine the Euler angles, θ and ϕ. Unfortunately, due to noise in the force measurements, smaller angles in the motions could not be determined conclusively. The angles that were able to be measured (Exp. Unop.) are shown in Table II along with their simulation counterparts (Sim. Unop.) for comparison.

The close agreement between simulation and experimental residual swing in the unoptimized cases speaks well for the accuracy of the ADAMS simulations. Though quantitative measurements of the optimized swing angles could not be obtained, we infer that the simulation accuracy extends to those cases as well. Qualitative observation of the residual swing for the optimized experimental runs did confirm that the residual motion was much smaller than the unoptimized cases.

Since practical application of the work will necessarily

TABLE II

RESIDUAL SWING AMPLITUDES: EXPERIMENTAL COMPARISON

(SIGNAL TO NOISE RATIOS IN OPTIMIZED TRAJECTORY RUNS WERE TOO SMALL TO DETERMINE ANGLES FROM FORCE MEASUREMENTS)

Traj.	Ang.	Exp. Unop. (deg)	Sim. Unop. (deg)	% Diff.
Short Poly. 2	θ	6.287	5.147	19.9
	ϕ	3.326	3.159	5.15
Long Poly. 1	θ	9.368	8.993	4.08
	ϕ	6.195	7.058	13.3
Long Poly. 2	θ	20.59	22.75	9.97

introduce uncertainty in the payload dynamics, the matter of the sensitivity of the method to these uncertainties naturally arises. We have not yet performed a systematic study to characterize the sensitivity, but the work to date does indicate that this is an issue of concern, and is a topic for future work.

IV. CONCLUSIONS AND FUTURE WORK

We have shown that dynamic programming can be successfully applied to curvilinear transport of suspended objects. Simulations showed an average 94.5% reduction in the residual swing angles between unoptimized and DP optimized maneuvers, with similar reductions experimentally. For trajectories comprised of splined segments, little error build-up was noticed during experimental verification.

Future work will include a closer look at trajectories comprised of multiple segments splined together, with the aim of eliminating acceleration discontinuities at via points. We may also examine spatial formulations other than elliptical arcs and polynomials and extend the work to the full three degree of freedom system. Finally, the sensitivity of the method to uncertainties in payload dynamics will be characterized.

V. ACKNOWLEDGMENTS

The authors would like to thank Dr. David Vick for his help in the experimental validation studies.

REFERENCES

[1] John J. Craig, *Introduction to Robotics: Mechanics and Control, 3rd Edition*, Prentice Hall, 2003, pp. 201-225.

[2] O.J.M. Smith, "Posicast Control of Damped Oscillatory Systems,", *Proceedings of the IRE*, pp. 1249-1255, 1957.

[3] G.P. Starr, "Swing-Free Transport of Suspended Objects with a Path-Controlled Robot Manipulator," *ASME Journal of Dynamic Systems, Measurement, and Control,* v.107, March 1985.

[4] D.R. Strip, "Swing-Free Transport of Suspended Objects: A General Treatment," *IEEE Transactions on Robotics and Automation,* v.5, n.2, April 1989.

[5] N.C. Singer and W.P. Seering, "Preshaping Command Inputs to Reduce System Vibration," *ASME Journal of Dynamic Systems, Measurement, and Control,* v.112, March 1990.

[6] W. Singhose, E. Crain, and W. Seering, "Convolved and Simultaneous Two-Mode Input Shapers," *IEE Proceedings - Control Theory and Applications*, v.144, n.6, pp. 515-520, November 1997.

[7] Kyung-Tae Hong, Chang-Do Huh, and Keum-Shik Hong, "Command Shaping Control for Limiting the Transient Sway Angle of Crane Systems," *International Journal of Control, Automation, and Systems*, v.1, n.1, pp. 43-53, March 2003.

[8] B.J. Petterson, R.D. Robinett, J.C. Werner, "Parameter-Scheduled Trajectory Planning for Suppression of Couples Horizontal and Vertical Vibrations in a Flexible Rod," *Proceedings, 1990 IEEE International Conference on Robotics and Automation*, May 1990.

[9] G.G. Parker, B. Petterson, C.R. Dohrmann, R.D. Robinett, "Vibration Suppression of Fixed-Time Jib Crane Maneuvers," Sandia National Laboratories report SAND95-0139C, 1995.

[10] G. Starr, J. Wood, and R. Lumia, "Rapid Transport of Suspended Objects," *2005 IEEE International Conference on Robotics and Automation*, Barcelona, Spain, April 18-22, 2005.

[11] R.E. Bellman, *Dynamic Programming*, Princeton University Press, New Jersey, 1957.

[12] R.D. Robinett, D.G. Wilson, G.R. Eisler, J.E. Hurtado, *Applied Dynamic Programming for Optimization of Dynamical Systems*, SIAM Advances in Design and Control, 2005.